Bull. Mater. Sci., Vol. 33, No. 4, August 2010, pp. 383–390. © Indian Academy of Sciences.

Temperature dependence of electromechanical properties of PLZT *x*/57/43 ceramics

A K SHUKLA*[,1,2], V K AGRAWAL[1], I M L DAS[1], JANARDAN SINGH[3] and S L SRIVASTAVA[1]

[1]Department of Physics, University of Allahabad, Allahabad 211 002, India
[2]Presently at Department of Physics, Amity School of Engineering & Technology, Amity University, Sec. 125, Noida, G. B. Nagar, UP, India
[3]National Physical Laboratory, Dr K S Krishnan Road, New Delhi 110 012, India

MS received 11 February 2009

Abstract. **The compositions of lead lanthanum zirconate titanate PLZT [$Pb(Zr_{0.57}Ti_{0.43})O_3 + x$ at% of La, where x = 3, 5, 6, 10 and 12] have been synthesized using mixed oxide route. The temperature dependent electromechanical parameters have been determined using vector impedance spectroscopy (VIS). The charge constant d_{31} and elastic compliance s_{11}^E show a peak in all the samples at a temperature T_{mt} much below the ferroelectric – paraelectric transition temperature, whereas the series resonance frequency f_s shows a dip at these temperatures. The Poisson's ratio σ^E increases with temperature T showing a broad peak at a temperature higher than T_{mt}. The voltage constant g_{31} decreases and the planar coupling coefficient K_p remains constant up to half of the T_{mt} and then falls sharply with T. Half of the T_{mt} can, therefore, be used for specifying the working temperature limit of the piezoceramics for the device applications.**

Keywords. **PLZT; MPB; vector impedance spectroscopy; electromechanical parameters.**

1. Introduction

La-doped lead zirconate titanate (PLZT) piezoelectric ceramics near the morphotropic phase boundary (MPB) region possessing high value of the electromechanical properties have found extensive use in various electromechanical, ultrasonic and underwater acoustic devices (Haertling 1999). The PLZT family also finds technological applications in the electrooptic and pyroelectric devices. Earlier studies revealed that the ceramic compositions having high piezoelectric strain can find their applications in emerging areas of micromechatronics, such as in camera installed cellular phones for auto focusing, cooling module for fuel cell power supply in laptops, optical fibre alignment, robotics, artificial fertilization system, micro pumps, drug delivery systems, ultrasonic distillations, injection valves and energy harvesting (Haertling 1999; Uchino 2008). The various compositions of PLZTs have shown excellent electromechanical properties that suited for such applications (Haertling 1999; Shukla *et al* 2004) and so, the functional properties of PLZTs have been extensively studied (Ochiai *et al* 1998; Bobnar *et al* 1999; Paik *et al* 1999; Kamba *et al* 2000; Volkov *et al* 2003; Tang *et al* 2007; Chen *et al* 2008). However, there has not been much systematic study of the temperature dependence of electromechanical properties of PLZT.

It has been observed that the compositions of PLZT ceramics with Zr/Ti 57/43 show enhanced piezoelectric response at room temperature and can be used in low power transducer devices (Shukla *et al* 2004). Keeping the device application in view, we have studied the temperature dependence of electromechanical properties of PLZT for different compositions. In the present work, we report effect of temperature on the electromechanical properties of compositions of PLZT of Zr/Ti 57/43 using vector impedance spectroscopy.

2. Experimental

The compositions of La doped PZT [$Pb(Zr_{0.57}Ti_{0.43})O_3 + x$ at% of La, where x = 3, 5, 6, 10 and 12] have been synthesized using mixed oxide route. The details of sample preparation and poling have been discussed by us earlier (Shukla *et al* 2004, 2006). The diameter 2a, thickness t, live capacitance, C_L and density of the synthesized samples are listed in table 1. The impedance and phase measurements of the disc shaped samples have been carried out using a computer controlled Solartron 1260 Impedance Gain Phase analyzer coupled with Solartron 1296 dielectric interface in the frequency range of 1 Hz – 1 MHz varying the temperature from room temperature (RT) to 400°C.

*Author for correspondence (akshukla@amity.edu)

3. Results and discussion

Variation of the magnitude of impedance, Z, with temperature and frequency for 3 at% La sample is shown in figure 1. The impedance spectra of all the fabricated samples of PLZT show that the temperature range of piezoelectric response decreases with increasing La concentration for the fundamental radial mode as well as for the overtones showing a decrease in the ratio Z_{max}/Z_{min} and Δf_{ps} ($= f_p - f_s$, where f_p and f_s are the parallel and series resonance frequencies). Z_{max} is the maximum impedance at the frequency, f_n and Z_{min} is the minimum impedance at the frequency, f_m. At f_s real part of $1/(\omega|Z(\omega)|)$ is maximum whereas at f_p the real part of $\omega|Z(\omega)|$ is maximum (Shukla *et al* 2004), where angular frequency $\omega = 2\pi f$. A typical plot of the variation of Z_{max}/Z_{min} of the fundamental radial mode with temperature, T, is given in figure 2. After a certain temperature, the values of Z_{max}/Z_{min} decrease rapidly with T, which depends on La concentration. On further increasing the temperature, the piezoelectric response disappears at the temperature much lower than the ferroelectric to paraelectric phase transition of the material. The same behaviour is observed for the overtones also. However, the piezoelectric response of the overtones disappears at a lower temperature than the fundamental mode.

The quantity, Δf_{ps}, depends on the electromechanical coupling coefficient as well as geometry of the piezoceramic material (Jaffe *et al* 1971). The behaviour of Δf_{ps} with T is shown in figure 3 and is similar to that of Z_{max}/Z_{min} for the fundamental mode (see figure 2).

The variation of series resonance frequencies, f_s, corresponding to the fundamental resonance mode is shown in figure 4. The values of f_s decrease with increase in La concentration except for La = 12·1 at% for which it increases. A similar behaviour of f_s with T has also been observed for the first and second overtones. It may also be noted that for each sample the series resonance frequency decreases up to a certain temperature beyond which they increase showing a broad minima, the broadening increases with the doping of La in the base PZT except for La = 12·1 at%. A similar temperature dependence in f_s has been reported for PZT systems close to the MPB region (Uchida and Ikeda 1967; Thomann 1972; Cheon and Park 1997; Zhang *et al* 1997), and also away from the MPB region (Dong and Kojima 1997). It has been shown that the temperature coefficient of resonant

Table 1. Geometrical parameters: diameter D, thickness t, live capacitance C_L and density ρ of different La doped PZT.

x (at%)	$2a$ (mm)	t (mm)	C_L (pF)	ρ (g/cm^3)
3·0	14·30	1·09	1·30	7·46
5·0	14·05	1·08	1·27	7·38
6·0	13·93	1·10	1·23	7·33
10·1	14·23	1·09	1·29	6·81
12·1	13·57	1·09	1·18	7·19

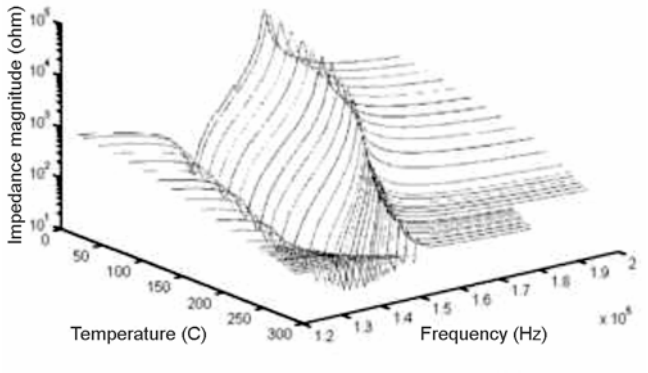

Figure 1. Variation of magnitude of impedance with temperature and frequency for x = 3·0 at% of La.

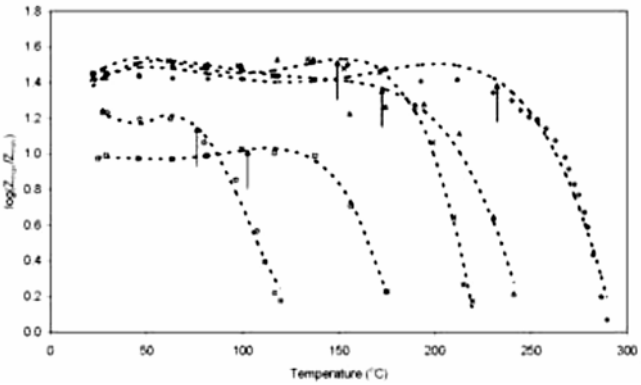

Figure 2. Variation of ratio of magnitude of maximum impedance to the minimum impedance for the fundamental radial mode corresponding to various compositions of PLZT. The symbols ◊, Δ, ×, □ and o correspond to x = 3·0, 5·0, 6·0, 10·1 and 12·1 at% of La.

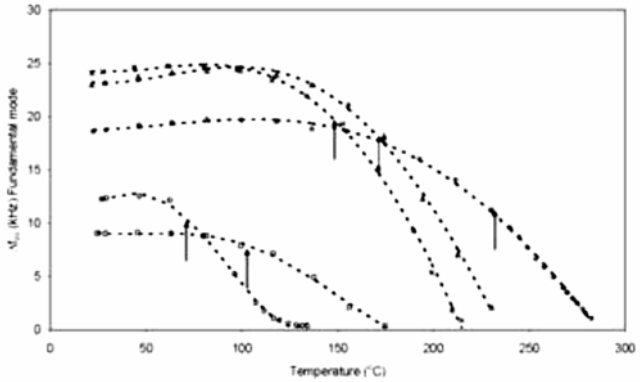

Figure 3. Change in difference of parallel and series resonance frequency Δf_{ps} for fundamental mode with temperature corresponding to different compositions of PLZT. The symbols ◊, Δ, ×, □ and o correspond to x = 3·0, 5·0, 6·0, 10·1 and 12·1 at% of La.

frequency is negative in the rhombohedral dominant phase and positive in the tetragonal phase (Heywang and Thomann 1984). It is known that at the room temperature PZT compositions in MPB region are in the mixed phase of rhombohedral and tetragonal phases in which rhombohedral phase is predominant and on heating they go to tetragonal phase (Heywang and Thomann 1984). As such the behaviour of resonance frequencies changing its slope with T from negative to positive sign may be a manifestation of the structural phase transition of the mixed rhombohedral – tetragonal phase to the tetragonal phase at T_{mt}. Such a broad phase transition has also been observed in Nb doped lead zirconate titanate (PZT), and attributed to the rhombohedral to tetragonal phase transition (Zhang *et al* 1997). The reason for a very large increase in f_s for x = 12·1 at% is anomalous.

The piezoelectric response has been simulated on the equivalent circuit shown in figure 5. The simulated circuit parameters R, L, C_a, C_b and R_b for the fundamental radial mode and first two overtones of PLZT at La 6 at% are presented in table 2. A similar behaviour is observed for the PLZT samples at x = 3, 5, 10 and 12 at%. R first decreases with T and then increases for the fundamental mode (see figure 6) as well as the first and second overtones. R increases with the overtones almost at all the temperatures. It may, however, be noted that at high temperatures the simulated parameters have large uncertainties because of very weak piezoelectric response. Inclusion of $R_b \| C_b$ does improve the simulation at high temperatures, and significantly for the overtones.

R in the equivalent circuit represents the mechanical loss of the piezoelectric response of the material and increase in R beyond a certain temperature indicates that the freezing of domains is disturbed and they become mobile due to the thermal agitation. This is supported by the increase in dielectric data with temperature, T (see figure 6(b)).

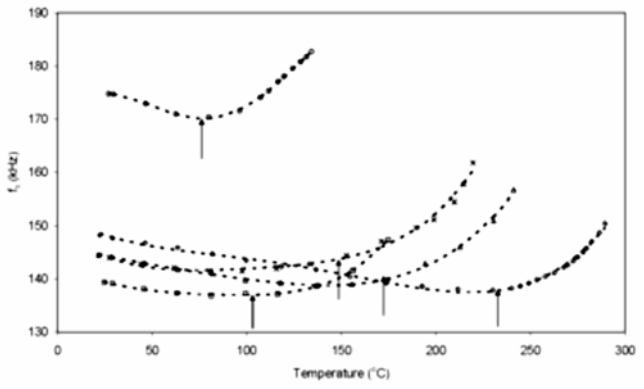

Figure 4. Temperature dependence of series resonance frequency for fundamental mode of various samples of PLZT. The symbols ◊, Δ, ×, □ and ○ correspond to x = 3·0, 5·0, 6·0, 10·1 and 12·1 at% of La.

Simulated values of L first decreases with T and beyond a certain T it starts increasing for the fundamental mode and the overtones, following almost the same behaviour as the simulated values of R. For the fundamental mode variation of L as a function of T is shown in figure 7. The increase in L at elevated temperatures is more pro-

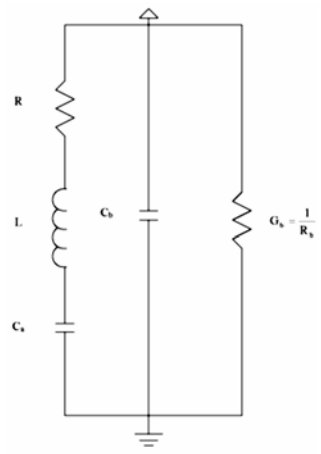

Figure 5. Piezoelectric equivalent circuit of single isolated piezoelectric resonance.

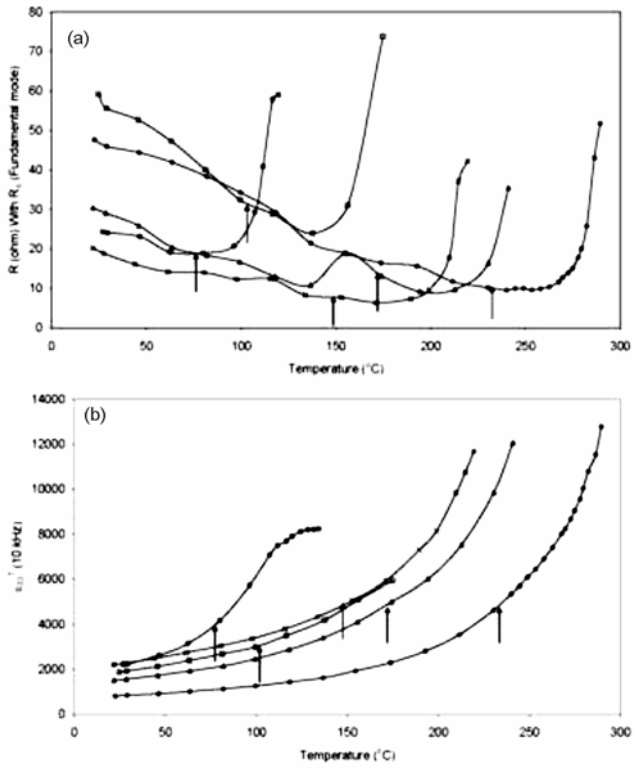

Figure 6. Variation of (**a**) equivalent circuit parameter R and (**b**) dielectric constant ε_{33}^T with temperature for various compositions of PLZT. The symbols ◊, Δ, ×, □ and ○ correspond to x = 3·0, 5·0, 6·0, 10·1 and 12·1 at% of La.

Table 2. Temperature dependence of different equivalent circuit parameters with R_b for the fundamental mode, first overtone and second overtone for x = 6 at% of La.

	Fundamental mode					First overtone					Second overtone				
Temperature (°C)	R (ohm)	L (mH)	C_a (pF)	C_b (nF)	R_b (kΩ)	R (ohm)	L (mH)	C_a (pF)	C_b (nF)	R_b (kΩ)	R (ohm)	L (mH)	C_a (pF)	C_b (nF)	R_b (kΩ)
21·75	20·2	1·74	697	1·93	∞	75·5	1·87	97	1·77	–	115	1·91	39	1·88	2·10
27·50	18·9	1·68	725	1·99	∞	73·7	1·80	102	1·83	∞	107	1·85	41	1·95	2·20
44·05	16·1	1·53	812	2·17	∞	65·1	1·64	113	1·99	∞	89	1·68	46	2·14	2·10
61·59	14·2	1·40	898	2·37	∞	54·3	1·52	125	2·19	∞	73	1·51	52	2·64	2·00
80·44	14·0	1·27	997	2·62	∞	46·9	1·38	138	2·44	∞	63	1·36	57	2·64	1·40
97·66	12·3	1·15	1100	2·94	∞	39·3	1·26	152	2·75	∞	55	1·28	63	2·89	1·40
115·83	12·4	1·07	1180	3·31	∞	35·7	1·16	166	3·13	∞	48	1·15	69	3·31	0·80
133·88	8·3	0·96	1300	3·93	∞	27·4	1·11	172	3·74	∞	39	1·00	79	4·00	0·70
152·75	7·7	0·90	1350	4·73	∞	22·8	0·99	190	4·63	∞	30	0·90	87	5·11	0·50
171·37	6·4	0·91	1290	5·96	∞	18·0	1·00	182	5·91	1·70	24	0·84	90	6·79	0·30
189·62	7·4	1·12	1010	7·89	∞	18·4	0·99	180	8·16	0·70	24	0·77	95	9·59	0·10
199·06	9·6	1·64	674	9·30	22	20·0	1·17	148	9·84	0·30	27	0·91	79	12·30	0·08
209·81	17·7	3·98	267	11·8	1·50	28·1	1·93	85	13·80	0·20	37	0·69	98	17·50	0·05
214·81	37·2	7·56	135	13·1	0·70	57·9	3·31	48	14·80	0·10	43	0·91	71	17·10	0·02
219·63	42·2	15·12	640	14·5	0·70										

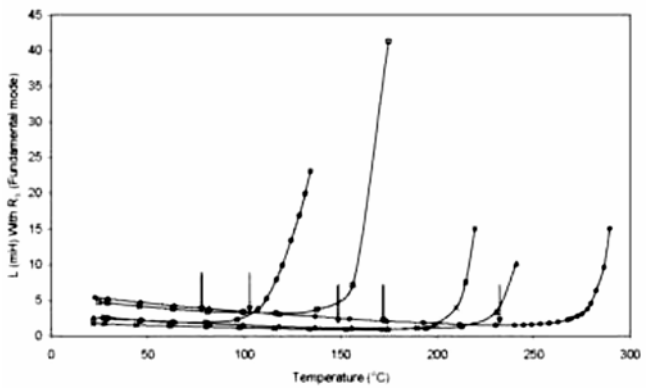

Figure 7. Change in inductance L of equivalent circuit with temperature for compositions of PLZT. The symbols ◊, Δ, ×, □ and o correspond to x = 3·0, 5·0, 6·0, 10·1 and 12·1 at% of La.

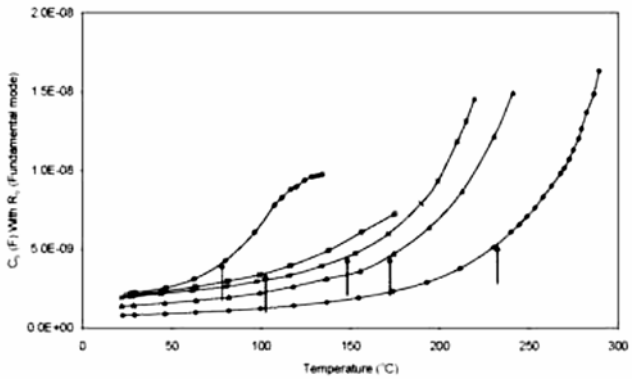

Figure 9. Temperature dependence of equivalent circuit parameter C_b for compositions of PLZT. The symbols ◊, Δ, ×, □ and o correspond to x = 3·0, 5·0, 6·0, 10·1 and 12·1 at% of La.

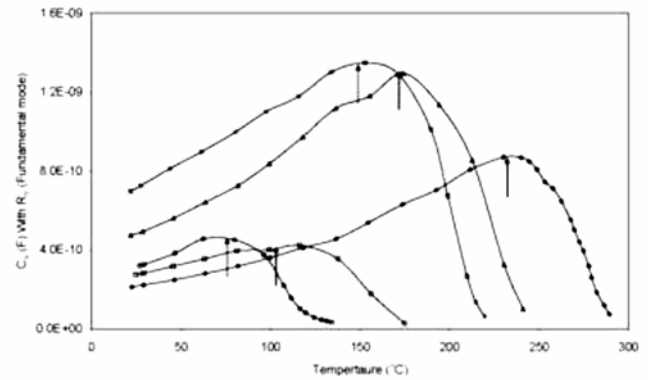

Figure 8. Trend of equivalent circuit parameter C_a with temperature for various samples of PLZT. The symbols ◊, Δ, ×, □ and o correspond to x = 3·0, 5·0, 6·0, 10·1 and 12·1 at% of La.

nounced for the fundamental mode than those for the first and second overtones. For a piezoelectric resonator, the value of L represents equivalent mass in the mechanical systems (Jaffe *et al* 1971), and a low value of L is a measure of good quality of the piezoelectric material (Katiyar *et al* 1994). In the present study the material with La at 6·0 at% has the lowest value of L below the temperature from which it rises and hence it should have better electromechanical properties compared to the other members of the series.

C_a increases with T up to a certain value, beyond which, it decreases sharply (see figure 8). C_a decreases with the overtones also. C_a, in the piezoelectric equivalent circuit, represents the elastic compliance s_{11}^E and the charge constant d_{31}, transformed into its electrical equivalent by the piezoelectric effect (Mason 1964; Jaffe *et al* 1971; Katiyar *et al* 1997).

The circuit parameter C_b represents the capacitance of the material under no resonance condition (Jaffe *et al* 1971). It is found that C_b remains almost same for the fundamental mode and overtones. C_b increases monotonically with T (see figure 9).

R_b (=1/G_b) is the shunt resistance in the equivalent circuit across C_b and the conductance G_b is a measure of the dielectric loss of the material in the absence of electromechanical resonance. For the fundamental mode, the values of R_b are found to be very large ($\sim 10^{20}$ Ω) up to a certain T. On further increase in T, the values of R_b fall. For the first and second overtones, values of R_b are in kΩ range in the entire temperature range (see table 2).

The variation of the oscillator figure of merit $M = (Q_m/r) = (1/\omega_s C_b R))$ with T for the fundamental radial mode is shown in figure 10. M shows a weak variation with temperature for all the samples and decreases after a certain temperature T_{mt}. The maximum value of M has been observed for x = 6·0 at%. The behaviour of M with T is a combined temperature dependent behaviour of mechanical quality factor, Q_m and capacitive ratio, $r = C_b/C_a$.

The electromechanical parameters Poisson's ratio σ^E, planar coupling coefficient K_P, transverse coupling coefficient K_{31}, elastic compliance s_{11}^E, piezoelectric charge constant d_{31} and voltage constant g_{31} have been calculated using the following equations (Shukla *et al* 2004).

$$\frac{K_p^2}{1-K_p^2} = \frac{\begin{pmatrix}(1-\sigma^E)J_1[\varphi(1+(\Delta f_{ps}/f_s))] \\ -\varphi(1+(\Delta f_{ps}/f_s))J_0[\varphi(1+(\Delta f_{ps}/f_s))]\end{pmatrix}}{(1+\sigma^E)J_1[\varphi(1+(\Delta f_{ps}/f_s))]},$$

$$\left(\frac{f_{si}}{f_{s0}}\right)^2 = (\varphi_i/\varphi_0)^2\left[\frac{1-(1/3)(\varphi_i\sigma^E t/(1-\sigma^E)2a)^2}{1-(1/3)(\varphi_0\sigma^E t/(1-\sigma^E)2a)^2}\right],$$

$$(1-\sigma^E)J_1(\varphi) = \varphi J_0(\varphi),$$

$$K_{31}^2 = 0{\cdot}5(1-\sigma^E)K_p^2,$$

$$\frac{1}{s_{11}^E} = \frac{4\pi^2 a^2 f_s^2(1-\sigma^{E^2})\rho}{\varphi^2},$$

$$d_{31} = K_{31}(\varepsilon_0\varepsilon_{33}^T s_{11}^E)^{1/2}$$

and

$$g_{31} = d_{31}/\varepsilon_0\varepsilon_{33}^T.$$

Symbols have their usual meanings.

Poisson's ratio σ^E gradually increases with T for each sample up to a certain maximum and a further increase in T results in a gradual decrease in σ^E (see figure 11). Such a behaviour in σ^E for Nb doped PZT near and away from the MPB region has also been reported earlier (Dong and Kojima 1997; Zhang *et al* 1997).

Variations of the electromechanical coupling coefficient K_P with T are shown in figure 12. K_p remains almost constant with T up to a certain value and then decreases. The decrease in K_p is of the diffuse type. A small increase in K_P for all the samples is observed below the temperature from which it starts to decrease. Several workers have also reported that the coupling coefficient, K_p, peaks at a temperature for PZT close and away to MPB, and also for lead titanate (Meitzler and O'Bryan 1973; Kim *et al* 1989; Dong and Kojima 1997; Zhang *et al* 1997; Bobnar *et al* 1999). However, a continuous decrease of K_{31} (K_p) with T followed by saturation for PLZT 8/65/35 has also been reported (Bobnar *et al* 1999).

The elastic compliance, s_{11}^E, increases gradually with T (see figure 13) and shows a peak at a certain T. The maximum value of s_{11}^E is observed for La composition of

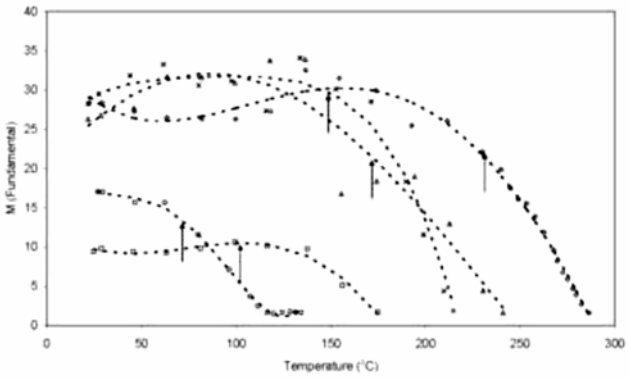

Figure 10. Variation of figure of merit M of the equivalent circuit with temperature for each composition of PLZT. The symbols ◊, Δ, ×, □ and ○ correspond to x = 3·0, 5·0, 6·0, 10·1 and 12·1 at% of La.

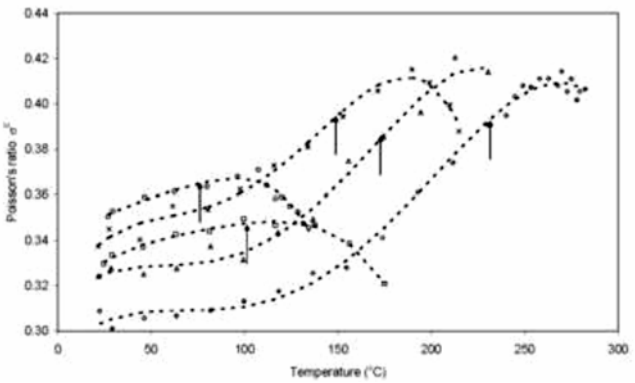

Figure 11. Variation of Poisson's ratio σ^E with temperature for different compositions of PLZT. The symbols ◊, Δ, ×, □ and ○ correspond to x = 3·0, 5·0, 6·0, 10·1 and 12·1 at% of La.

x = 10·1 at%. Meitzler and Bryan (1973) reported a sharp peak in s_{11}^E with temperature for PLZT 7·2/65/35, whereas Bobnar *et al* (1999) observed a broad maximum in s_{11}^E for PLZT 8/65/35. Zhang *et al* (1997) reported that temperature dependence of shear modulus of PZT near MPB region exhibits a broad minimum around the phase coexistence region.

The variation of strain constant or charge constant, d_{31}, is shown in figure 14. d_{31} also shows a peak at a certain T for all samples. A maximum of d_{31} is found for La composition of x = 6·0 at%.

The voltage constant, g_{31}, decreases with both T and La dopant concentration as shown in figure 15. This is in conformity with the dominating tetragonal structure over the rhombohedral phase at $T > T_{mt}$, because 'g' values are maximum in the rhombohedral side (Jaffe *et al* 1971).

It has been observed that the electromechanical properties of piezoceramics degrade with temperature and hence the maximum working temperature limits of these materials are required to be known for their use in fabrication of the transducer devices. In general, half of the temperature, T_m, at which the dielectric constant of piezoceramics becomes maximum is considered safe for device application (Turner *et al* 1994). Also the temperature coefficients of various dielectric and electromechanical constants are important in predicting the behaviour of the piezoceramic materials particularly those which have a high electromechanical coupling (IEEE Standards on Piezoelectricity 1987). The electromechanical parameters of presently studied compositions could be fitted on a fourth order polynomial using the method of least square (IEEE Standards on Piezoelectricity 1987)

$$X = X_{ref}\left[1+\sum_{n=1}^{4} a_n (\Delta T)^n\right],$$

where $\Delta T = T - T_{ref}$. The X_{ref} and T_{ref} correspond to the room temperature. The coefficients a_n, for various para-

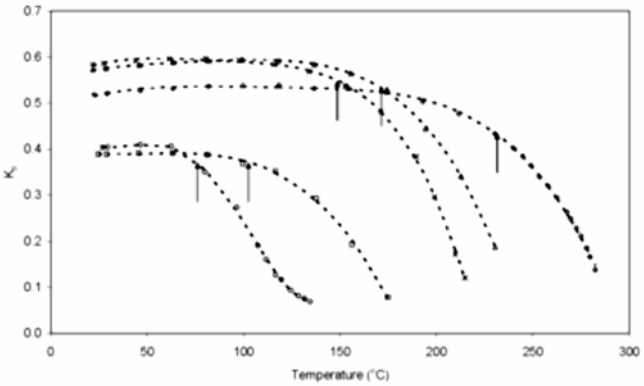

Figure 12. Temperature dependence of planar coupling coefficient K_P for various PLZT samples. The symbols ◊, Δ, ×, □ and o correspond to x = 3·0, 5·0, 6·0, 10·1 and 12·1 at% of La.

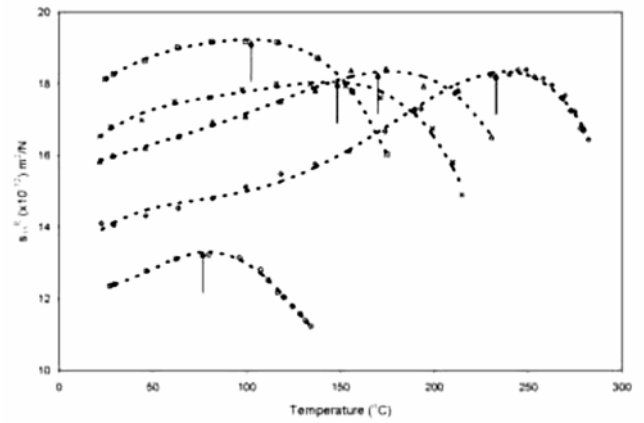

Figure 13. Temperature dependence of elastic compliance s_{11}^E for PLZT compositions. The symbols ◊, Δ, ×, □ and o correspond to x = 3·0, 5·0, 6·0, 10·1 and 12·1 at% of La.

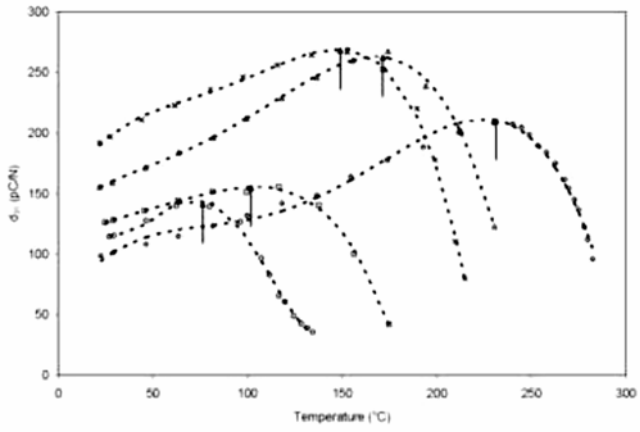

Figure 14. Variation of strain constant d_{31} with temperature for PLZTs. The symbols ◊, Δ, ×, □ and o correspond to x = 3·0, 5·0, 6·0, 10·1 and 12·1 at% of La.

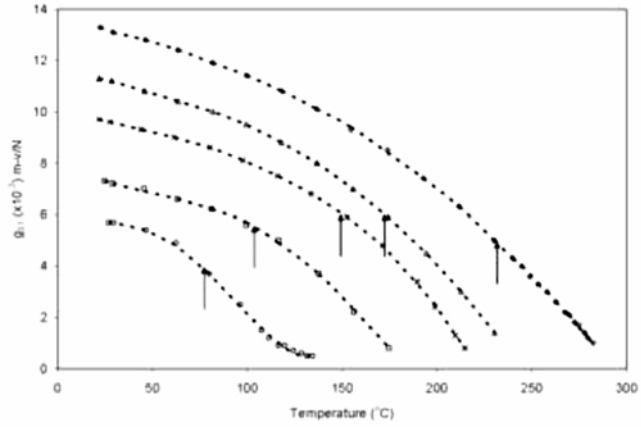

Figure 15. Temperature dependence of voltage constant g_{31} for different compositions of PLZT x/57/43. The symbols ◊, Δ, ×, □ and o correspond to x = 3·0, 5·0, 6·0, 10·1 and 12·1 at% of La.

Table 3. Normalized temperature coefficients of 4th order polynomial fit of various electromechanical parameters of 6 at% of La.

	x = 6·0 at% of La			
	a_1 ($\times 10^{-3}$/°C)	a_2 ($\times 10^{-5}$/°C^2)	a_3 ($\times 10^{-7}$/°C^3)	a_4 ($\times 10^{-10}$/°C^4)
$\log(Z_{max}/Z_{min})$	7·50	–22·70	22·90	–73·50
f_s	–1·10	1·94	–1·48	4·61
Q_m	–8·60	27·80	–26·80	87·90
M	4·50	–8·62	8·32	–32·70
σ^E	2·00	–4·52	5·20	–16·50
K_p	2·20	–5·79	6·12	–24·90
K_{31}	1·80	–5·06	5·12	–21·20
s_{11}^E	2·50	–3·99	3·47	–11·50
d_{31}	8·20	–14·60	16·00	–59·50
g_{31}	–1·40	–1·10	0·48	–4·19

Table 4. Values of T_{mt} determined by the variation of s_{11}^E and d_{31} with T, thermal depoling temperature, T_d and ferroelectric phase transition temperature, T_m, for compositions of PLZT.

	x = 3·0 at% T_{mt} (°C)	x = 5·0 at% T_{mt} (°C)	x = 6·0 at% T_{mt} (°C)	x = 10·1 at% T_{mt} (°C)	x = 12·1 at% T_{mt} (°C)
s_{11}^E ($x10^{-12}$)m^2/N	238	176	148	101	79
d_{31} (pC/N)	225	168	149	104	73
Average T_{mt} (°C)	232 ± 7	172 ± 2	148·5 ± 0·5	102·5 ± 2·5	76 ± 3
T_d (°C)	292	245	222	180	137
T_m (°C)	300	256	233	196	143

meters, for 6 at% of La are listed in table 3. The fitted curves of $\log(Z_{max}/Z_{min})$, Δf_{ps}, f_s, M, σ^E, K_p, s_{11}^E, d_{31} and g_{31} are shown by dotted lines in the respective plots.

It is clear from the above study that there exist two distinct regions of various electromechanical parameters with T for the compositions of PLZT under investigation. Such a change in material constants of PLZT has been observed by Tang *et al* (2007), who have attributed this to the ferroelectric rhombohedral – tetragonal phase transition. The low temperature phase transition is a common feature of poled PZT close to the MPB region (Heywang and Thomann 1984; Cordero *et al* 2007; Tang *et al* 2007; Pandey *et al* 2008; Singh *et al* 2008).

The charge constant (also known as the strain constant) of a piezoelectric crystal is given by

$$d = \frac{\partial S}{\partial E} = \frac{\partial D}{\partial T'},$$

where S is the strain, E the applied electric field, D the dielectric displacement and T' the stress (Jaffe *et al* 1971). Through vector impedance spectroscopy we apply an electric field, E, which for the piezoelectric materials produces the strain 'S', which in turn results in the stress T'. The elastic compliance, $s_{11}^E = (\partial S/\partial T')_E$ and 'd' may, therefore, be more appropriate electromechanical parameters for the determination of the temperature, T_{mt}, which may represent the phase transition from the mixed rhombohedral – tetragonal phase to the tetragonal phase. These temperatures are listed in table 4 and arrows on different curves correspond to the average T_{mt}. The gradual change, either of decreasing or increasing nature in each electromechanical property is observed through the mixed rhombohedral – tetragonal phase transition to the tetragonal phase transition. It may be noted that all these phenomena are happening below the ferroelectric – paraelectric phase transitions. As such all the electromechanical properties diminish below the ferroelectric – paraelectric phase transition temperature at which the macroscopic polarization in the material is lost due to the thermal depoling. This temperature is known as the thermal depoling temperature, T_d; which is listed in table 4 along with the ferroelectric phase transition temperature T_m. It has been further observed that the $T_{mt} < T_d < T_m$.

4. Conclusions

The piezoelectric materials based on the PLZT x/57/43 are systematically investigated at elevated temperature by using VIS technique. The various electromechanical parameters are determined and fitted on a fourth order polynomial using the method of least square.

The electromechanical parameters of La doped PZT at a characteristic temperature T_{mt} suggests a structural phase transition from rhombohedral – tetragonal to

tetragonal phase below the ferroelectric – paraelectric phase transition. This is evidenced mainly by the behaviour of d_{31} and s_{11}^E with temperature. As such the charge constant 'd' and elastic compliance s_{11}^E may be the appropriate parameters in determination of phase transition temperature, T_{mt}, by VIS technique.

As no appreciable variation in the piezoelectric coupling coefficients, K_p and K_{31}, has been observed within half of the T_{mt}, hence it would be safe to use these piezoelectric materials as transducer element within half of the T_{mt} for low power transducer devices.

Acknowledgements

One of us (AKS) is thankful to the Council of Scientific and Industrial Research (CSIR), New Delhi, for the grant of a Senior Research Fellowship. (AKS) gratefully acknowledges Dr Ashok K Chauhan, Amity University, Uttar Pradesh, for his support.

References

Bobnar V, Kutnjak Z and Levstik A 1999 *J. Eur. Ceram. Soc.* **19** 1281
Cheon C and Park J S 1997 *J. Mater. Sci. Lett.* **16** 2043
Chen Y T, Lin S C and Cheng S Y 2008 *J. Alloys Compd* **449** 101
Cordero F, Cracium F and Galassi C 2007 *Phys. Rev. Lett.* **98** 255701
Cross L E 1994 *Ferroelectrics* **151** 305
Dong X and Kojima S 1997 *Jpn J. Appl. Phys.* **36** 2989
Haertling G H 1999 *J. Am. Ceram. Soc.* **82** 797
Heywang W and Thomann H 1984 *Ann. Rev. Mater. Sci.* **14** 27
IEEE Standards on Piezoelectricity 1987 (ANSI/IEEE Std, 176)
Jaffe B, Cook W R and Jaffe H 1971 *Piezoelectric ceramics* (London: Academic Press)
Kamba S, Bovtun V, Petzelt J, Rychetsky I, Mizaras R, Brilingas A, Banys J, Grigas J and Cosec M 2000 *J. Phys.: Condens. Matter* **12** 497
Katiyar V K, Srivastava S L and Singh J 1994 *J. Appl. Phys.* **76** 455
Katiyar V K, Srivastava S L and Singh J 1997 *Ferroelectrics* **193** 21
Kim J N, Haun M J, Jang S J, Cross L E and Xue X R 1989 *IEEE Trans. UFFC* **36** 389
Mason W P 1964 *Physical acoustics – Principles and methods* (New York: Academic Press)
Meitzler A H and O'Bryan Jr H M 1973 *Proc. IEEE* **61** 959
Ochiai T, Yokosuka M, Mitsuhashi H, Koyama S and Sasaki Y 1998 *Jpn J. Appl. Phys.* **37** 6077
Pandey D, Singh A K and Baik S 2008 *Acta Crystallogr.* **A64** 192
Paik D S, Park S E, Shrout T R and Hackenberger W 1999 *J. Mater. Sci.* **34** 469
Singh A K, Mishra S K, Ragini, Pandey D, Yoon S, Baik S and Shin N 2008 *Appl. Phys. Lett.* **92** 022910
Shukla A K, Agrawal V K, Soni N C, Singh D P, Singh J and Srivastava S L 2004 *Ferroelectrics* **308** 67
Shukla A K, Agrawal V K, Das I M L, Singh J, Singh D P and Sood K N 2006 *Phase Trans.* **79** 875
Tang B, Fan H, Ke S and Liu L 2007 *Mater. Sci. & Eng.* **B138** 205
Thomann H 1972 *Ferroelectrics* **4** 141
Turner R C, Fuierer P A, Newnham R E and Shrout T R 1994 *Appl. Acoust.* **41** 299
Uchino K 2008 *J. Electroceram.* **20** 301
Uchida N and Ikeda T 1967 *Jpn J. Appl. Phys.* **6** 1292
Volkov A A, Ritus A I and Khvalkovskii A V 2003 *Ferroelectrics* **285** 219
Zhang S, Dong X and Kojima S 1997 *Jpn J. Appl. Phys.* **36** 2994